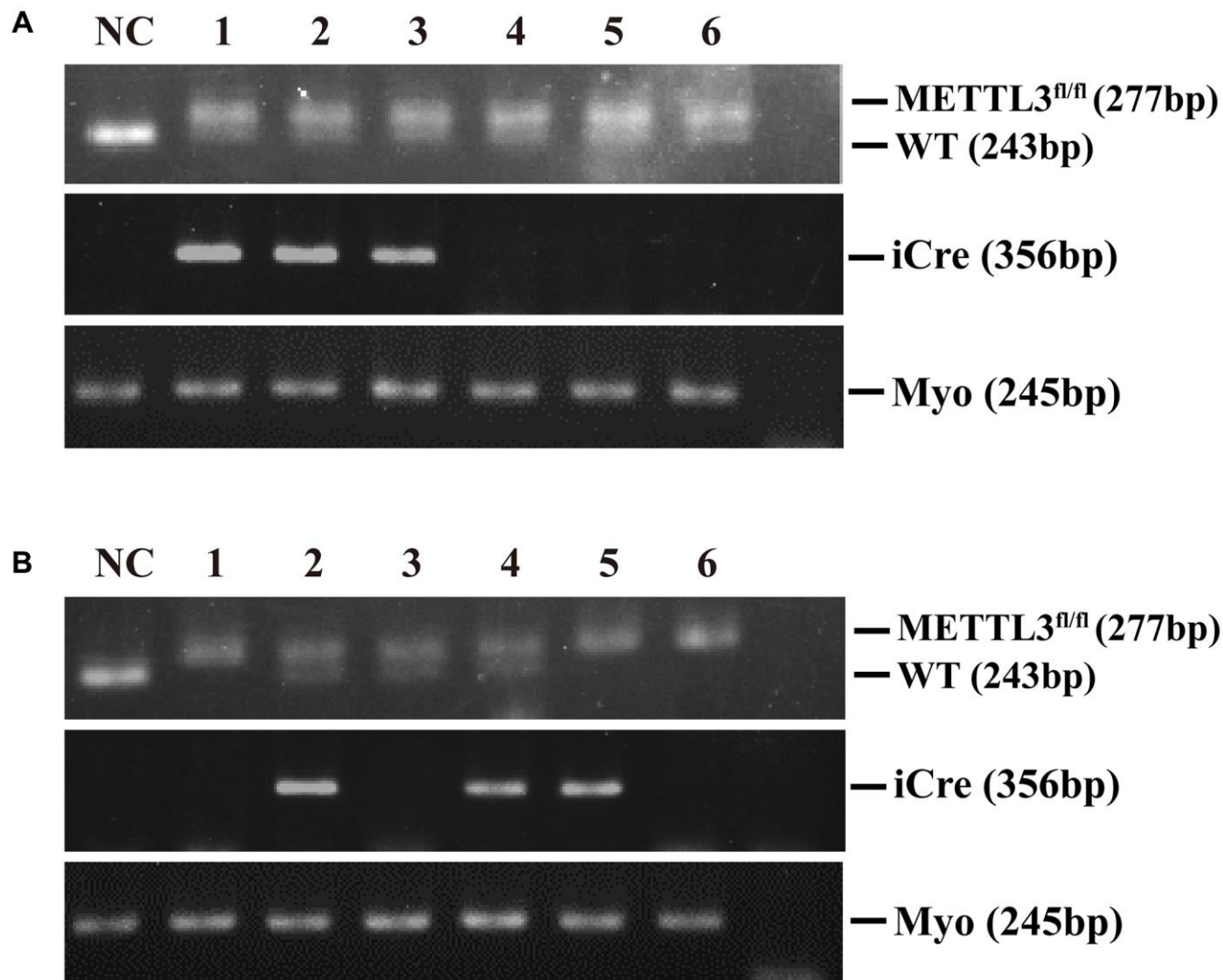
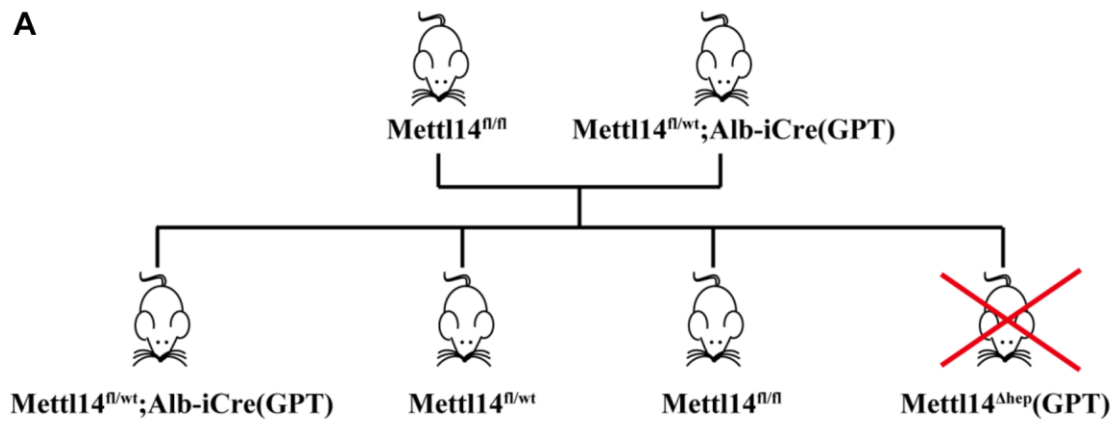


**SUPPLEMENTARY FIGURES**



**Supplementary Figure 1. PCR-based genotyping of hepatocyte-specific METTL3 homozygous knockout (METTL3<sup>Δhep</sup>) mice by Alb-iCre mice (GPT).** (A) PCR-based genotyping displays the offspring with indicated genotypes from intercrossing METTL3<sup>fl/fl</sup> mice and Alb-iCre (GPT) mice. (B) PCR-based genotyping exhibits the offspring with indicated genotypes from intercrossing METTL3<sup>fl/fl</sup> mice and METTL3<sup>fl/wt</sup>; Alb-iCre (GPT) mice.

**A**



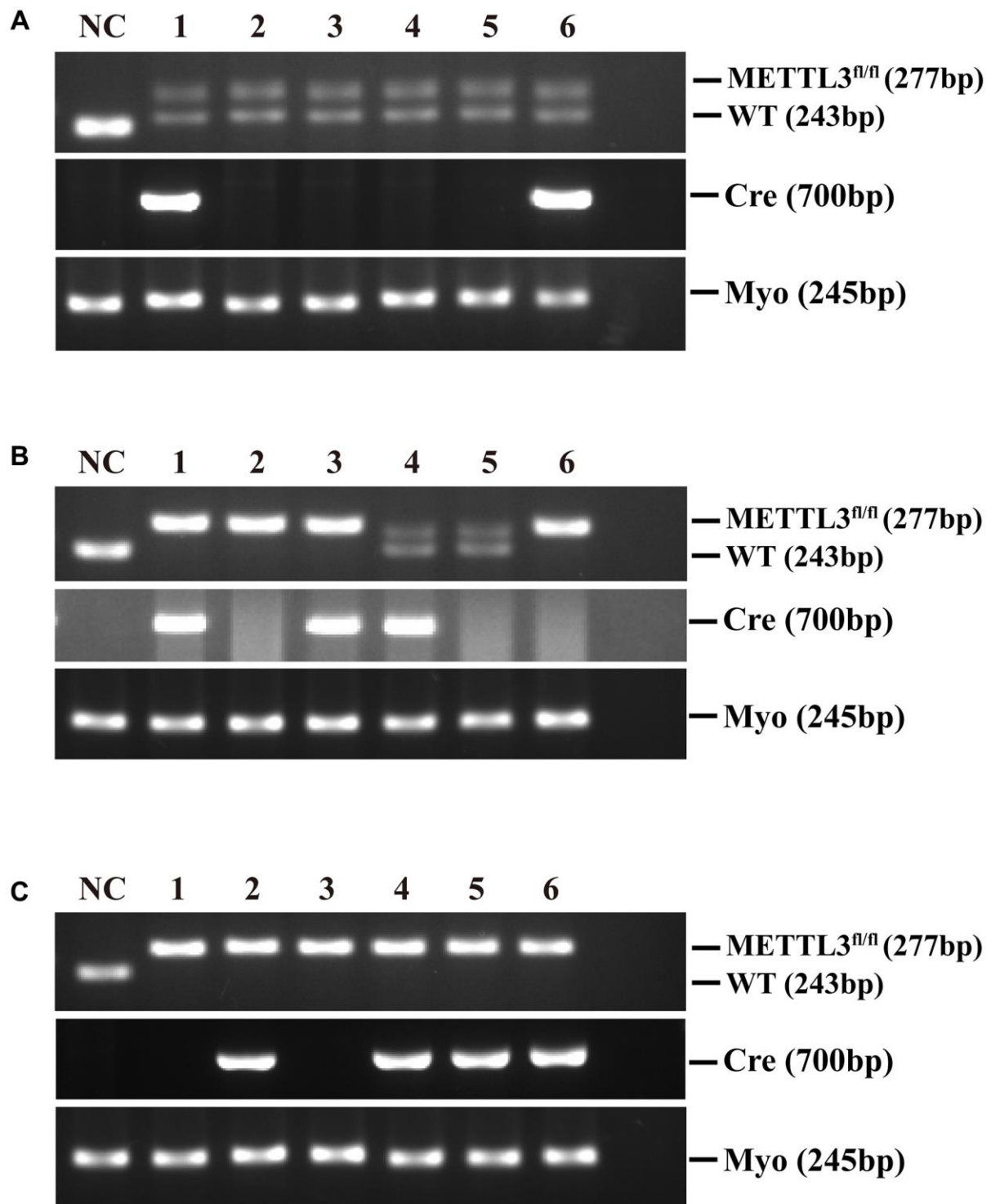
**B**

Genotype	Number	Ratio (%)
$Mettl14^{fl/wt}$	15	38.46
$Mettl14^{fl/wt}; Alb-iCre(GPT)$	12	20.77
$Mettl14^{fl/fl}$	12	30.77
$Mettl14^{\Delta hep}(GPT)$	0	0
<b>Total</b>	<b>39</b>	

**C**

Genotype	Number	Ratio (%)
$Mettl14^{fl/wt}$	6	28.57
$Mettl14^{fl/wt}; Alb-iCre(GPT)$	6	28.57
$Mettl14^{fl/fl}$	5	23.81
$Mettl14^{\Delta hep}(GPT)$	4	19.05
<b>Total</b>	<b>21</b>	

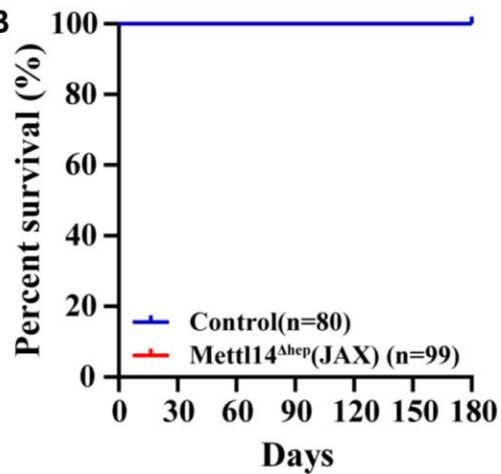
**Supplementary Figure 2. Hepatocyte-specific METTL14 homozygous ablation in mice by Alb-iCre mice (GPT) results in postnatal lethality.** (A) A schematic representation of the offspring with indicated genotypes from intercrossing  $METTLL14^{fl/fl}$  and  $METTLL14^{fl/wt}; Alb-iCre (GPT)$  mice. (B) PCR-based genotyping during the late postnatal period displays the number of offspring with indicated genotypes from intercrossing  $METTLL14^{fl/fl}$  mice and  $METTLL14^{fl/wt}; Alb-iCre (GPT)$  mice. (C) PCR-based genotyping during the early postnatal period exhibits the number of offspring with indicated genotypes from intercrossing  $METTLL14^{fl/fl}$  mice and  $METTLL14^{fl/wt}; Alb-iCre (GPT)$  mice.



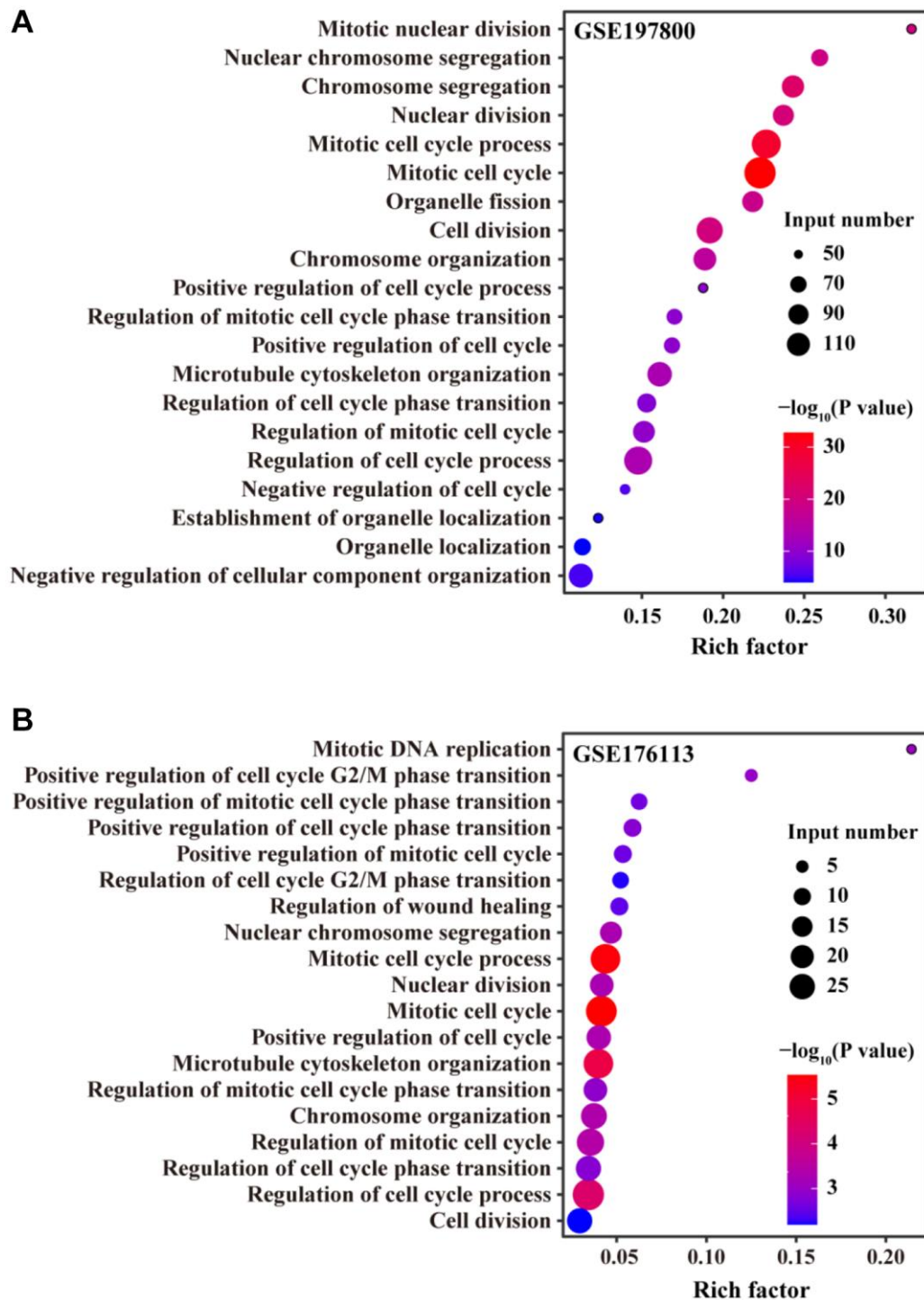
**Supplementary Figure 3. PCR-based genotyping of hepatocyte-specific METTL3 homozygous knockout (METTL3<sup>Δhep</sup>) mice by Alb-Cre mice (JAX).** (A) PCR-based genotyping displays the offspring with indicated genotypes from intercrossing METTL3<sup>fl/fl</sup> mice and Alb-Cre (JAX) mice. (B) PCR-based genotyping exhibits the offspring with indicated genotypes from intercrossing METTL3<sup>fl/fl</sup> mice and METTL3<sup>fl/wt</sup>; Alb-Cre (JAX) mice. (C) PCR-based genotyping exhibits the offspring with indicated genotypes from intercrossing METTL3<sup>fl/fl</sup> mice and METTL3<sup>fl/fl</sup>; Alb-Cre (JAX) mice.

**A**

Genotype	Number	Ratio (%)
Control	80	44.69
Mettl14 <sup>Δhep</sup> (JAX)	99	55.31
Total	179	

**B**

**Supplementary Figure 4. Hepatocyte-specific ablation of METTL14 in mice by Alb-Cre mice (JAX) didn't lead to postnatal lethality.** (A) PCR-based genotyping during the late postnatal period shows the presence of offspring with the genotype (i.e., METTL14<sup>fl/fl</sup>; Alb-Cre (JAX): referred to as METTL14<sup>Δhep</sup> (JAX)) from intercrossing METTL14<sup>fl/fl</sup> mice and METTL14<sup>fl/fl</sup>; Alb-Cre (JAX) mice. (B) Survival curves of control and METTL14<sup>Δhep</sup> (JAX) mice ( $n = 80-99$  for each group).



**Supplementary Figure 5.** GO term enrichment analyses of up-regulated DEGs (from RNA-seq data deposited in GEO under accession number GSE197800 (A) and GSE176113 (B)) in the liver of control and METTL3<sup>Δhep</sup> (JAX) mice.